Mon. Not. R. astr. Soc. (1985) **214,** 379–398

Cloud fragmentation and stellar masses

Richard B. Larson *Astronomy Department, Yale University, PO Box 6666, New Haven, Connecticut 06511, USA*

Accepted 1985 January 3. Received 1985 January 2; in original form 1984 October 26

Summary. Theoretical arguments and numerical simulations both suggest that a star-forming cloud generally collapses to a flattened or filamentary configuration before fragmenting, and that fragmentation occurs as a result of the gravitational instability of the resulting layer or filament. A number of existing and new results for the stability of polytropic sheets, discs, and filaments are collected in this paper, and critical lengths and masses are derived for a variety of values of the polytropic exponent. The critical mass varies as T^2/μ, where T is the temperature and μ the surface density of the fragmenting cloud; the numerical coefficient is approximately the same for both sheets and filaments. Rotation and magnetic fields tend to inhibit fragmentation, but they do not fundamentally change the characteristic length and mass scales involved.

The predictions of these stability analyses agree satisfactorily with the results of numerical simulations of the fragmentation of discs and filaments. The predicted critical masses in some well-studied regions of star formation also agree with the typical masses of the observed dense cloud clumps, and, in order of magnitude, with the masses of the young stars present. Differences in the observed fragment masses in different regions can be understood as due primarily to differences in the gas temperature, which is the dominant parameter controlling the mass scale for fragmentation. Fragmentation to smaller masses is likely to continue during the early stages of cloud evolution when the temperature decreases with increasing density, but it becomes less likely and may stop altogether when the temperature reaches its minimum value; this may produce a peak in the stellar initial mass function at the corresponding mass. The typical stellar mass should then increase strongly with increasing minimum cloud temperature.

1 Introduction

Present evidence suggests that the initial mass function (IMF) for stars in the solar vicinity has nearly a power-law form for large masses but deviates from this form for masses below one solar mass, reaching a peak at a few tenths of a solar mass and then declining rapidly toward smaller masses (Scalo 1985a, b). Some clusters and associations may contain relatively fewer low-mass stars, so that in these regions the IMF may peak at a larger mass. With a peaked IMF, the bulk of

the mass goes into stars whose mass is near that of the peak, which therefore is a characteristic mass for star formation. A major problem for the theory of star formation is then to understand the origin of this characteristic mass and the factors determining it.

In order to understand the origin of stellar masses, it is first necessary to understand the relation between the mass of a star and that of the cloud condensation in which it forms. Larson (1984) has argued that the efficiency of star formation in a protostellar condensation will be high because gravitational torques will redistribute angular momentum outward until most of the mass has condensed into a star or binary system. As a result, there should be a close relationship between the mass of a star and the mass of its progenitor cloud condensation. Observations confirm that the masses of newly formed stars and the masses of the associated dense clumps in molecular clouds are indeed of the same order; for example, in the Taurus dark clouds, T Tauri stars with a typical mass of $\sim 0.5\,M_\odot$ are seen in close association with dense cloud cores whose typical mass is $\sim 0.7\,M_\odot$ (Myers & Benson 1983; see Section 6). The problem of understanding stellar masses then becomes, in essence, the problem of understanding the masses of the observed clumps in molecular clouds.

The observed clumpy structure of molecular clouds is almost certainly a result of gravity, the sizes of the smallest clumps reflecting an approximate balance between gravity and pressure. The classical Jeans (1929) analysis of fragmentation by gravitational instability predicts a critical mass, the 'Jeans mass', such that density enhancements containing more mass can grow with time. This mass decreases with increasing density, so it is possible in principle for condensations of progressively smaller mass to develop in a cloud that is undergoing overall contraction. Hoyle (1953) accordingly proposed, in an influential paper, that stars form by the fragmentation of a cloud into a hierarchy of progressively smaller condensations as it collapses. The original Jeans analysis, however, neglects the overall collapse of the medium in which the density perturbations are embedded; this overall collapse actually tends to overwhelm the collapse of finite-sized density perturbations, whose development is retarded by pressure gradients (see Section 2.1). Thus it is not clear that fragmentation can actually occur in this situation, and this queston has been a subject of debate (Layzer 1963; Hunter 1964).

As a result of much recent numerical work, it has become clear that fragmentation during near free-fall collapse is indeed an inefficient process; fragmentation can become significant only if large density perturbations are present initially, small perturbations tending to be damped out during the collapse (e.g. Tohline 1980a, b; Rozyczka 1983). In a cloud with rotation or initial flattening, fragmentation becomes marked only after the cloud has collapsed to a highly flattened disc-like configuration. Tohline (1980a, b) has suggested that fragmentation occurs primarily as a result of the instability and break-up of such near-equilibrium discs. Supporting this suggestion, Wood (1982) and Miyama, Hayashi & Narita (1984) have noted that in their numerical collapse simulations, fragmentation occurs in discs and in approximate accordance with the criterion for disc stability of Goldreich & Lynden-Bell (1965a). The likely relevance of disc instabilities to fragmentation was noted earlier by Larson (1972), and indeed Jeans (1929) had suggested that rotationally supported discs would provide a favourable environment for star formation in galaxies.

In Sections 2 and 3 of this paper, it will be seen that the essential property of a disc that favours fragmentation is its flattening, not its rotation, since a non-rotating equilibrium gas sheet (or filament) fragments in much the same way. A number of other effects besides rotation, including a magnetic field and initial anisotropy, can also cause a cloud to collapse to a flattened or filamentary configuration (Mestel 1965). Molecular clouds may even be formed with sheet-like structures from the outset, for example by interstellar shocks or cloud collisions (Smith 1980). A one-dimensional collapse or compression process is always eventually halted by increasing pressure forces, and as a result an equilibrium gas sheet is formed. Similarly, if $\gamma > 1$,

two-dimensional compression leads to the formation of an equilibrium filament. In either case, the balance between pressure and gravity establishes a scale height that constitutes a natural dimension for the system and provides a characteristic length scale for fragmentation.

In contast to the mathematically questionable Jeans analysis for an infinite uniform medium, a rigorous stability analysis is possible for equilibrium sheets and filaments, and it is readily seen that fragmentation is not jeopardized by the overall collapse of the medium. Instead, density perturbations of a well-defined characteristic size and mass grow more rapidly than others and become well separated. At the same time, because the system as a whole does not collapse, the possibilities for extensive hierarchical fragmentaton are much more limited than in the Hoyle picture. Fragmentation is thus likely to produce objects with a limited range of masses and a well-defined characteristic mass, as would be required to account for a peaked IMF.

In this paper we adopt the basic assumption that the fragmenting regions of molecular clouds have approached hydrostatic equilibrium in at least one dimension, or that they will do so at an early stage of star formation. In Section 2 we present a compilation of results, existing and new, for the stability of polytropic gas sheets and filaments, with particular attention to the values of γ that are most relevant to fragmenting clouds. The effects of rotation and magnetic fields on the stability of self-gravitating sheets and filaments are summarized in Section 3. In Section 4, the theoretical predictions are compared with the results of numerical simulations, and in Section 5 the thermal behaviour of dense interstellar clouds is reviewed and critical masses for fragmentation are derived. Comparisons with observations of regions of star formation are made in Section 6, and some limitations on continuing fragmentation, and their implications for the form of the IMF, are discussed in Section 7.

2 Critical lengths and masses for fragmentation

In this section we present in a common framework a number of existing and new results for the gravitational stabilty of equilibrium gas sheets and filaments; for comparison, we also include some results for an infinite uniform medium. We consider not only the usual isothermal equation of state but also several non-isothermal equations of state, including in particular the cases with $\gamma<1$ that are most relevant for fragmenting clouds (see Section 5). We assume that the equation of state can be modelled by the simple polytropic law

$$P=K\varrho^{\gamma}=K\varrho^{1+1/n}. \tag{1}$$

Since thermal equilibrium time-scales are nearly always much shorter than dynamical time-scales, we assume that the same temperature–density relation holds for both the equilibrium state and the dynamical perturbations to be studied. Rotation, turbulence, and magnetic fields are neglected here, but the effects of rotation and magnetic fields on stability will be reviewed in Section 3.

2.1 INFINITE UNIFORM MEDIUM

Although this case is not likely to be realistic, we recall and extend slightly for comparison with other cases the results of the classical Jeans (1929) analysis of the gravitational stability of an infinite uniform medium. For plane-wave density perturbations with time and space dependence given by $\exp(i\omega t)\cos kx$, the dispersion relation relating ω^2 to k is

$$\omega^2=\gamma c^2k^2-4\pi G\varrho. \tag{2}$$

Here and throughout the paper, c denotes the isothermal sound speed $(P/\varrho)^{1/2}$. The same dispersion relation holds for spherically symmetric density perturbations with a spatial

dependence of the form $r^{-1}\sin kr$. In either case, there is a critical wavenumber

$$k_c=(4\pi G\varrho/\gamma c^2)^{1/2} \tag{3}$$

such that for smaller wavenumbers ω^2 is negative and growth occurs. For spherically symmetric modes, a critical mass M_c can be defined as the mass in the contracting region interior to the first minimum of the function $r^{-1}\sin k_c r$; this mass is

$$M_c=8.53\gamma^{3/2}c^3/G^{3/2}\varrho^{1/2}. \tag{4}$$

This is similar to the 'Jeans mass' $M_J=5.57\gamma^{3/2}c^3/G^{3/2}\varrho^{1/2}$, as derived more heuristically by assuming plane-wave perturbations (e.g. Spitzer 1978).

For comparison with later results, it will be convenient to write the dispersion relation (2) in dimensionless form by defining a length scale $H=(c^2/4\pi G\varrho)^{1/2}$, a time-scale $\tau=H/c$, a dimensionless growth rate $\Omega=i\omega\tau$, and a dimensionless wavenumber $\nu=kH$; equation (2) then becomes

$$\Omega^2=1-\gamma\nu^2. \tag{5}$$

It is immediately apparent from equation (5) why the instability of an infinite uniform medium is not a very effective mechanism of fragmentation: the growth rate Ω increases monotonically with decreasing wavenumber ν and is a maximum for $\nu=0$, i.e. for an infinite wavelength; thus the fastest growing mode is an overall contraction of the medium. Consequently, fragmentation can become significant only if sufficiently large density enhancements are present initially, or if they are created by non-gravitational processes during the collapse (Tohline 1980b).

2.2 INFINITELY THIN SHEET

While again not realistic in detail, infinitely thin sheets have often been used to model galactic discs, and they show in a simple way the same qualitative behaviour as gas layers of finite thickness. For an infinitely thin sheet with surface density μ, the dispersion relation for surface-density perturbations of the form $\exp(i\omega t)\cos kx$ is

$$\omega^2=\gamma c^2k^2-2\pi G\mu k. \tag{6}$$

The same dispersion relation holds for circularly symmetric perturbations with a spatial dependence given by the Bessel function $J_0(kr)$. We can write equation (6) in dimensionless form by defining a length scale $H=c^2/\pi G\mu$, and defining again $\Omega=i\omega H/c$ and $\nu=kH$; we then obtain

$$\Omega^2=2\nu-\gamma\nu^2. \tag{7}$$

As in the Jeans problem, there is a critical wavenumber

$$k_c=2\pi G\mu/\gamma c^2, \quad \text{or} \quad \nu_c=2/\gamma \tag{8}$$

such that modes with wavenumber smaller than k_c or wavelength larger than $\lambda_c=2\pi/k_c$ grow with time. For modes with circular symmetry, the critical mass M_c may be defined as the mass in the contracting region interior to the first minimum of the function $J_0(k_c r)$; this gives

$$M_c=1.17\gamma^2c^4/G^2\mu. \tag{9}$$

A major qualitative difference from the Jeans problem is evident in the form of the dispersion relation (7): the growth rate Ω has a maximum at a finite wavenumber $\nu=\nu_c/2$, i.e. at a wavelength $\lambda=2\lambda_c$, and decreases to zero as $\nu\to 0$ or $\lambda\to\infty$. Thus fragmentation is not affected by an overall collapse of the medium, and modes with wavelength $2\lambda_c$ can grow faster than modes of

both shorter and longer wavelength, leading to clear fragmentation with a characteristic length scale $2\lambda_c$. The corresponding mass scale for the fastest growing mode is $4M_c$.

2.3 SELF-GRAVITATING ISOTHERMAL SHEET

The vertical density distribution in a self-gravitating equilibrium isothermal gas layer is given by

$$\varrho(z)=\varrho(0)\,\mathrm{sech}^2(z/H) \tag{10}$$

where the scale height H is defined by $H=\mu/2\varrho(0)=c^2/\pi G\mu$ (Spitzer 1942, 1978). For density perturbations having a horizontal spatial dependence of the form $\cos kx$ or $J_0(kr)$, the marginal mode with $\omega=0$ has been found analytically by Ledoux (1951; see also Spitzer 1978), and the resulting critical wavenumber is

$$k_c=\pi G\mu/c^2=H^{-1}, \quad \text{or} \quad \nu_c=1, \tag{11}$$

i.e. exactly half that for an infinitely thin sheet with $\gamma=1$. The critical mass, defined for circularly symmetric modes as the mass interior to the first minimum of the Bessel function $J_0(k_c r)$, is

$$M_c=4.67c^4/G^2\mu. \tag{12}$$

The dispersion relation for an isothermal sheet has been calculated numerically by Simon (1965) and is shown in Fig. 1, which plots Ω^2 versus ν, where again $\Omega=i\omega H/c$ and $\nu=kH$. The resulting curve is approximately an inverted parabola passing through the origin, and thus it is very similar, apart from a scale factor, to the dispersion relation for an infinitely thin sheet given by equation (7). Thus an isothermal sheet of finite thickness should fragment in qualitatively the same way as an infinitely thin sheet.

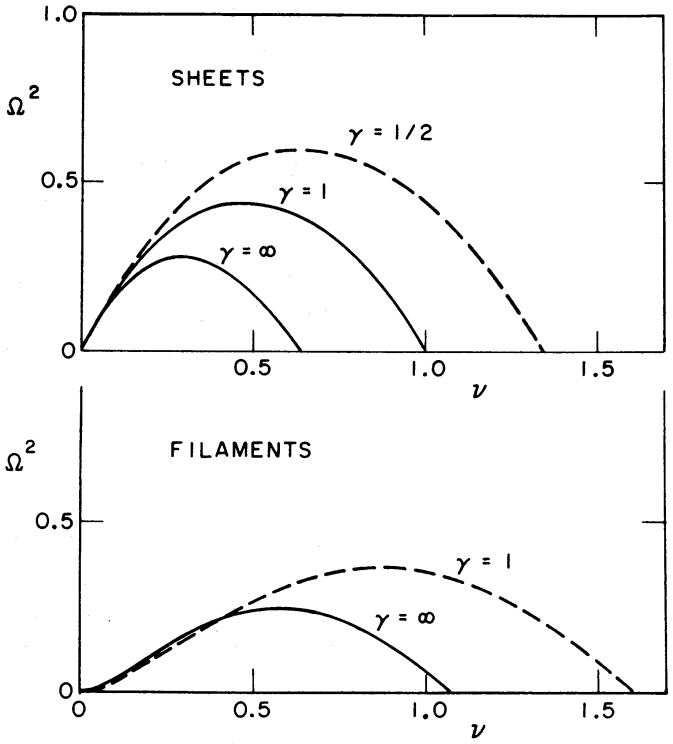

Figure 1. Dispersion relations for growing modes in polytropic sheets and filaments; the dimensionless squared growth rate Ω^2 is plotted versus the dimensionless wavenumber ν. For sheets, $\Omega=i\omega H/c(0)$ and $\nu=kH$, where H is defined by equation (14); for filaments, $\Omega=i\omega R/c(0)$ and $\nu=kR$, where R is defined by equation (20). The dashed curves are approximate dispersion relations estimated on the basis of scaling, as described in Sections 2.4 and 2.5.

An accurate analytic approximation to the dispersion relation which will be useful for further applications can be derived using the 'vertical equilibrium approximation' of Goldreich & Lynden-Bell (1965a, b), which neglects the inertia of the relatively small motions in the vertical direction. The result, in the present notation, is

$$\Omega^2 \cong 2\nu(1-\nu)/[1+\nu+(\nu^2/2)\,\zeta(\nu/2,2)] \equiv F(\nu). \tag{13}$$

The error in this approximation is less than 4 per cent in ω^2, or 2 per cent in ω.

The Ledoux–Simon analysis has been extended to pressure-bounded isothermal gas layers by Elmegreen & Elmegreen (1978). Although we shall not consider this situation here, we note that very similar dispersion relations are obtained even in this case, and the characteristic wavelength for fragmentation is still governed by the thickness of the compressed layer.

2.4 POLYTROPIC SHEETS

Polytropic sheets with $\gamma=2$ and $\gamma=\infty$ have been studied by Goldreich & Lynden-Bell (1965a), and a more general study of polytropic sheets has been made by Harrison & Lake (1972), who gave analytic solutions for the structure of sheets with $\gamma>1$. For the fragmentation problem, values of γ in the range $1/2\lesssim\gamma\lesssim1$ are most relevant (see Section 5); therefore we present here some new results for the structure and stability of sheets with $\gamma=1/4$, $1/2$, and $2/3$. We include also some results for $\gamma=2$ and ∞.

For polytropic sheets, we define a scale height H by

$$H=\mu/2\rho(0)=c(0)^2/\pi G\mu, \tag{14}$$

where $\rho(0)$ and $c(0)=[P(0)/\rho(0)]^{1/2}$ are quantities measured in the central plane $z=0$; this definition is valid for any equation of state. With the substitutions $z=yH$ and $\rho(z)/\rho(0)=\theta^n$, the equation of hydrostatic equilibrium and the Poisson equation for a plane-parallel layer can be combined to yield the dimensionless structure equation

$$d^2\theta/dy^2=-2\theta^n/(n+1). \tag{15}$$

An analytic solution for the density distribution exists for $\gamma=2/3$ $(n=-3)$, which is $\rho(z)=\rho(0)(1+z^2/H^2)^{-3/2}$. For $\gamma=1/2$ and $\gamma=1/4$, solutions of equation (15) have been calculated numerically.

To derive the marginal modes we assume, following Ledoux (1951), that the perturbation in the gravitational potential has a spatial dependence of the form $\psi(z)\cos k_c x$ or $\psi(z)J_0(k_c r)$. We also assume that the perturbations in pressure and density obey the same equation of state as the unperturbed structure. We then obtain the following eigenvalue equation for ψ:

$$d^2\psi/dy^2+(2\theta^{n-1}/\gamma-\nu_c^2)\,\psi=0. \tag{16}$$

The eigenvalue $\nu_c=k_cH$ is determined by the requirement that $\psi\rightarrow0$ as $y\rightarrow\infty$. For $\gamma=2$ and $\gamma=\infty$, the eigenvalue problem can be solved analytically in terms of trigonometric functions; for other values of γ, the eigenfunctions and eigenvalues have been found by numerical integration of equation (16). The resulting eigenvalues, ranging from $\nu_c=1.857$ for $\gamma=1/4$ to $\nu_c=0.639$ for $\gamma=\infty$, are tabulated in Table 1. The corresponding critical masses can be expressed as a function of $c(0)$ and μ by the relation

$$M_c=A(\gamma)\,c(0)^4/G^2\mu, \tag{17}$$

which is analogous to equation (12) for the isothermal case. The numerical coefficient $A(\gamma)$ in equation (17) varies from 1.36 for $\gamma=1/4$ to 11.4 for $\gamma=\infty$, and is also listed in Table 1.

Table 1. Critical wavenumbers and masses.

	Sheets			Filaments		
γ	k_cH	$A(\gamma)$	$B(\gamma)$	k_cR	$A(\gamma)$	$B(\gamma)$
1/4	1.857	1.36	1.70			
1/2	1.343	2.59	3.25			
2/3	1.182	3.35	4.19			
1	1.000	4.67	5.86	1.595	7.88	6.28
2	0.804	7.23	9.06	1.152	5.04	4.29
∞	0.639	11.44	14.34	1.067	3.75	3.32

The critical mass can be expressed alternatively, by analogy with the Jeans mass, as a function of $c(0)$ and $\varrho(0)$ by the relation

$$M_c=B(\gamma)c(0)^3/G^{3/2}\varrho(0)^{1/2}, \tag{18}$$

where the numerical coefficient $B(\gamma)$ is given in Table 1. For values of γ near 1/2, $B(\gamma)$ has nearly the same value as the coefficient $8.53\gamma^{3/2}$ in the analogous equation (4) for the critical mass in an infinite uniform medium.

For the incompressible case $\gamma=\infty$, the dispersion relation has the analytic form

$$\Omega^2=[1+\exp(-2\nu)-2\nu]\tanh\nu \tag{19}$$

(Goldreich & Lynden-Bell 1965a), where $\Omega=i\omega H/c(0)$ and $\nu=kH$. A pressure-confined gas layer exhibits effectively incompressible behaviour in the limit of large external pressure, and the results of Elmegreen & Elmegreen (1978) reproduce the above dispersion relation in this limit. This dispersion relation, shown in Fig. 1, is again very similar to those for the infinitely thin and isothermal cases, differing from them nearly by constant scale factors. It therefore seems likely that the dispersion relations for all values of γ will be very similar in form, differing essentially by scale factors. The dashed curve in Fig. 1 shows the dispersion relation for $\gamma=1/2$ as estimated on this basis by scaling the curve for $\gamma=1$ by the ratio of the values of k_cH in Table 1.

2.5 POLYTROPIC AND ISOTHERMAL FILAMENTS

While theoretical arguments suggest that self-gravitating clouds should generally collapse to flattened configurations, observations suggest that many dark clouds actually have elongated or filamentary shapes (Schneider & Elmegreen 1979). The origin of the observed filaments is not understood, but one possibility noted by Schneider & Elmegreen is that they have formed by the break-up of sheets. In any event, the dark filaments studied by Schneider & Elmegreen often show evidence for fragmentation into clumps, and in some cases young stellar objects are closely associated with the clumps. Thus it is of interest to examine the gravitational stability of cylindrical filaments, just as was done for gas sheets.

The structure of polytropic and isothermal cylinders has been studied by Ostriker (1964, 1965), and stability analyses have been carried out for the incompressible case by Chandrasekhar & Fermi (1953) and for the isothermal case by Stodolkiewicz (1963). A cylinder with $\gamma<1$ is unstable to radial collapse, so only values of $\gamma\geqslant1$ will be considered here. We note that even if the gas has $\gamma<1$, the effective value of γ in the radial direction may be >1 if the filament is partially supported by a magnetic field. In this section we present results for $\gamma=1$, 2, and ∞.

In the cylindrical case it is convenient to define a length scale H by $H=[K/2\pi G\varrho(0)^{1-1/n}]^{1/2}$. The density distributions for $\gamma=1$ and $\gamma=2$ then have the analytic forms $\varrho(r)\propto(1+r^2/4H^2)^{-2}$ and $\varrho(r)\propto J_0(r/H)$ (Ostriker 1964). Proceeding as before, we find that the marginal mode satisfies an eigenvalue equation that has the same form as equation (16) except for the addition of a term

$d\psi/ydy$ on the left-hand side. For $\gamma=1$, θ^{n-1} in equation (16) is replaced by $\varrho(r)/\varrho(0)$. The eigenvalues determined numerically for $\gamma=1$ and $\gamma=2$ are $k_cH=0.798$ and $k_cH=0.729$, the former value being in agreement with the previous result of Stodolkiewicz (1963). The value of k_cH obtained analytically by Chandrasekhar & Fermi (1953) for $\gamma=\infty$ is 0.754.

A scale radius R for a filament can also be defined in terms of the mass per unit length m by a relation analogous to the definition $H=\mu/2\varrho(0)$ used for the scale height of a sheet; we thus define

$$R=[m/\pi\varrho(0)]^{1/2}. \tag{20}$$

The quantity $\nu_c=k_cR$ varies from 1.595 for $\gamma=1$ to 1.067 for $\gamma=\infty$, and is tabulated in Table 1. The critical mass M_c is equal to $\lambda_c m$, where $\lambda_c=2\pi/k_c$. To compare the resulting critical masses with the values previously given for sheets, we express the critical mass in the two alternative forms

$$M_c=A(\gamma)c(0)^4/G^2\mu(0) \tag{21}$$

$$M_c=B(\gamma)c(0)^3/G^{3/2}\varrho(0)^{1/2} \tag{22}$$

analogous to equations (17) and (18); here $\mu(0)$ is the maximum surface density measured through the centre of the filament. The values of $A(\gamma)$ and $B(\gamma)$ for filaments are listed in Table 1.

From Table 1 we see that for values of γ between 1 and 2, the coefficient $A(\gamma)$ is approximately the same for filaments as for sheets. Thus when the critical mass for a cloud is calculated from its central temperature and its maximum surface density, the result is approximately the same whether the cloud is a sheet or a filament. A knowledge of the actual 3-dimensional structure of the cloud is therefore not crucial for predicting the critical mass, as long as it can be assumed that the cloud has approached hydrostatic equilibrium in at least one dimension.

The dispersion relation for an incompressible cylinder is

$$\Omega^2=2\nu I_1(\nu)[2K_0(\nu)-I_0(\nu)^{-1}] \tag{23}$$

(Chandrasekhar & Fermi 1953), where here $\Omega=i\omega R/c(0)$ and $\nu=kR$. This dispersion relation is plotted in the lower panel of Fig. 1, and it is again seen to be similar in general form to the results for plane-parallel sheets shown in the upper panel. In particular, the growth rate Ω has a maximum at a wavenumber of about $\nu_c/2$ and decreases to zero as $\nu\rightarrow 0$ or $\lambda\rightarrow\infty$, in this case even more rapidly than for sheets. The corresponding mass of the most rapidly growing mode is only about $2M_c$, so the range of mass scales for fragmentation is more narrowly defined than for sheets.

Since the dispersion relation for an incompressible sheet was found to be quite representative for the compressible case, apart from a scale factor, we expect this to be qualitatively true for filaments as well. An approximate dispersion relation for an isothermal filament, estimated by scaling the dispersion relation for $\gamma=\infty$ by the ratio of the values of ν_c, is shown by the dashed curve in the lower panel of Fig. 1.

3 Effects of rotation and magnetic fields

We now consider the effects of rotation and magnetic fields on the stability of self-gravitating sheets and filaments, particularly on the characteristic length and mass scales involved. It will be seen that rotation and magnetic fields reduce the growth rate and the range of wavelengths of unstable modes, but as long as instability is not suppressed completely, the basic length and mass scales are not substantially altered and are still determined essentially by the thickness of the fragmenting sheet or filament.

3.1 ROTATION

Rotation influences the growth of perturbations through the presence of an additional restoring force, the Coriolis force, which depends on the epicyclic frequency $\varkappa$. If the inertia of motions in

the vertical direction can be neglected, the dispersion relation for perturbations in a uniformly rotating gas layer, or for short-wavelength axisymmetric perturbations in a differentially rotating disc, is modified only by the addition of $\varkappa^2$ to ω^2. For example, the dispersion relation for non-shearing modes, including ring modes, in an infinitely thin disc is

$$\omega^2=\gamma c^2k^2-2\pi G\mu k+\varkappa^2 \tag{24}$$

(Hunter 1972). Defining

$$Q=c\varkappa/\pi G\mu, \tag{25}$$

where Q is the analogue of the Toomre (1964) stability parameter for a gas disc, equation (24) takes the dimensionless form

$$\Omega^2=2\nu-\gamma\nu^2-Q^2. \tag{26}$$

This differs from equation (7) only by the addition of the term $-Q^2$ on the right-hand side. Instability is completely suppressed if $Q>Q_c=\gamma^{-1/2}$, while for $Q<Q_c$ there is a range of unstable wavelengths, the most rapidly growing mode having the same wavelength as in the non-rotating case.

Using the vertical equilibrium approximation of Goldreich & Lynden-Bell (1965a, b), an analogous equation can be derived for the more realistic case of a self-gravitating isothermal disc of finite thickness; the result is

$$\Omega^2\cong F(\nu)-Q^2, \tag{27}$$

where $F(\nu)$ is defined in equation (13). Again, for non-shearing modes, the effect of rotation is just to reduce the dimensionless squared growth rate Ω^2 by a constant amount Q^2, without changing the wavelength of the fastest growing mode.

The vertical equilibrium approximation and hence equation (27) become exact when $\omega\rightarrow 0$, so we can use this equation to determine the critical value of Q for which instability is completely suppressed; the result is that instability is suppressed if Q exceeds the value $Q_c=0.676$. Similar results are obtained for non-isothermal discs if we define $Q=c(0)\varkappa/\pi G\mu$; since the dispersion relations without rotation differ nearly by constant scale factors, the critical value Q_c for stability varies approximately as $\nu_c^{1/2}$. For $\gamma=2$ and $\gamma=\infty$, the exact values of Q_c can be determined in the same way as for $\gamma=1$, using dispersion relations derived in the vertical equilibrium approximation (Goldreich & Lynden-Bell 1965a); the resulting values of Q_c are 0.597 and 0.526, agreeing to within 3 per cent with the approximate values found by scaling from $\gamma=1$.

In the incompressible case this local stability analysis reproduces with good accuracy the criterion for the ring instability of a Maclaurin spheroid. For a flattened Maclaurin spheroid, Q is independent of radius and is given in terms of the eccentricity e by

$$Q=\{12e^{-2}[e^{-1}(1-2e^2/3)(1-e^2)^{1/2}\arcsin e-1+e^2]\}^{1/2}. \tag{28}$$

From this relation, the value $Q_c=0.526$ predicted for $\gamma=\infty$ corresponds to an eccentricity of 0.99875, or to an axial ratio of 20.0. This is almost the same as the axial ratio of 21.5 at which the ring instability occurs in a Maclaurin spheroid (Bardeen 1971).

A compressible equation of state allows ring formation and fragmentation to occur in a less flattened system; for example, the critical value $Q_c=0.676$ predicted for an isothermal sheet corresponds to an axial ratio of 10.9 for a Maclaurin spheroid, or 13.0 for the centrally condensed isothermal disc models of Toomre (1982) and Hayashi, Narita & Miyama (1982). From numerical experiments, Hayashi *et al.* (1982) found that ring formation in these isothermal discs occurs approximately when $Q<0.75$, or when the axial ratio exceeds about 10.5. Non-axisymmetric fragmentation occurs at essentially the same value of Q as ring formation, according to the

simulations of Miyama *et al.* (1984). When $Q=0.75$, the predicted wavelength of the fastest growing mode at each radius is about twice the radius; thus an isothermal disc can fragment only if the fastest growing wavelength is smaller than the diameter. The existence of this requirement for the fragmentation of discs sets an important constraint on continuing fragmentation when rotation is important, as will be seen in Section 7.

For shearing, spiral-shaped perturbations in a differentially rotating disc, $\varkappa^2$ is replaced by a time-dependent quantity $\tilde{\varkappa}^2$ that is generally smaller than $\varkappa^2$ (Toomre 1981). As a result, shearing modes are generally less inhibited by rotation than non-shearing modes, and spiral perturbations can grow by large, although finite, factors even in cases where non-shearing perturbations are stable (Goldreich & Lynden-Bell 1965b; Toomre 1981). Thus there is an intermediate regime of 'incipient instability' between stability and classical instability, in which transient spiral disturbances can experience significant growth; this occurs for values of Q between about 2/3 and 4/3, the growth factor depending strongly on Q (Larson 1984).

It is noteworthy that, in all of the cases that have been discussed, even for shearing perturbations, the characteristic wavelength of the fastest growing mode is always given by $kH\sim 1/2$, just as in the non-rotating case. Thus, while rotation exerts an inhibiting effect on the fragmentation of gas sheets, the inhibiting effect is basically scale-independent and leaves unchanged the wavelength of the fastest growing mode. Therefore, if fragmentation can occur at all, the characteristic length and mass scales will be essentially the same as in the non-rotating case.

3.2 MAGNETIC FIELDS

In the presence of a strong magnetic field, a self-gravitating cloud will contract along the field lines and form a flat layer or disc threaded by a magnetic field perpendicular to its plane (e.g. Nakano 1984). The vertical structure of such a layer is not affected by the field, but the magnetic field constrains motions in its plane. As in the case of a rotating disc, the vertical equilibrium approximation can be used to derive an accurate analytic approximation to the dispersion relation. For the isothermal case, the stability analysis of Nakano & Nakamura (1978) yields the approximate dispersion relation

$$\Omega^2 \cong F(\nu) - p^2 G(\nu) \tag{29}$$

where $F(\nu)$ is given by equation (13),

$$G(\nu) = 2\nu/[1-\nu+(\nu^2/2)\,\zeta(\nu/2,2)], \tag{30}$$

and the magnetic stability parameter p (Nakamura 1983) is defined by

$$p^2 = B^2/4\pi^2 G\mu^2 = P_{\rm mag}/P_{\rm gas}(0). \tag{31}$$

Instability is suppressed if $p>1$, while for $p<1$ growing modes exist for wavenumbers less than a critical wavenumber given approximately by

$$\nu_{\rm c} = k_{\rm c} H \cong 1-p. \tag{32}$$

Thus, compared to the non-magnetic case, the critical wavelength is increased by approximately a factor $(1-p)^{-1}$ and the critical mass is increased by a factor $(1-p)^{-2}$. Again the dispersion relation has the same qualitative form as those shown in Fig. 1, the effect of a non-zero magnetic field being very similar to the effect of an increase in γ.

If both rotation and a perpendicular magnetic field are present, their effects on the dispersion relation are additive in the vertical equilibrium approximation, and we can combine equations (27) and (29) to obtain, for non-shearing perturbations in an isothermal disc,

$$\Omega^2 \cong F(\nu) - p^2 G(\nu) - Q^2 \tag{33}$$

(Nakamura 1983, 1984). Nakamura (1984) has calculated the exact dispersion relation for the special case $p^2=0.1$ and $Q^2=0.2$, and has found that it is approximated by equation (33) to an accuracy better than 2 per cent. The wavenumber of the fastest growing mode in this case is given by $kH=0.38$.

A magnetic field parallel to a gas layer is less effective than a perpendicular field in stabilizing the layer. For example, in an isothermal gas layer in which the ratio $P_{\rm mag}/P_{\rm gas}=p^2$ is constant, the critical wavelength for perturbations propagating perpendicular to the field is increased by a factor $1+p^2$ for a given temperature and surface density (Pacholczyk 1963). This is a weaker dependence on B than the factor $(1-p)^{-1}$ found above. For perturbations propagating along the field, the critical wavelength is increased by a factor $(1+p^2)(1+2p^2)^{-1/2}$, which is very close to unity for $p<1$ (Stodolkiewicz 1963).

For a filament with a longitudinal magnetic field, the dispersion relation in the incompressible case (Chandrasekhar & Fermi 1953) is

$$\Omega^2=2\nu I_1(\nu)[2K_0(\nu)-I_0(\nu)^{-1}]-2p^2\nu^2 \tag{34}$$

where $p^2=P_{\rm mag}/P_{\rm gas}(0)$. The critical wavelength varies approximately as $(1-p)^{-1}$ for small p and increases exponentially for $p>1$, effectively removing the instability for large p. For an isothermal magnetic filament with $P_{\rm mag}/P_{\rm gas}=p^2=$constant, the critical wavelength and mass again both increase with p for a given gas temperature and maximum surface density, the critical mass varying approximately as $1+1.2p^2$ for $p<1$ (Stodolkiewicz 1963).

Summarizing, the effect of a magnetic field is always stabilizing, the effect being greatest for a sheet threaded by a perpendicular magnetic field. In this case the critical mass and the mass of the fastest growing mode are both increased by approximately a factor $(1-p)^{-2}$, and instability is suppressed completely if $p>1$. Unless the magnetic field is almost strong enough to suppress gravitational instability altogether, the increase in the characteristic mass scale for fragmentation is only of order unity, so it should still be valid at least approximately to use the results derived for the non-magnetic case.

4 Comparison with simulations

Before comparing the above predictions with observations of regions of star formation, we compare them with the results of numerical simulations of cloud collapse and fragmentation. We restrict attention to simulations that clearly show fragmentation taking place in a flattened or filamentary configuration, and in which the initial conditions have not been chosen to favour a specific mode of fragmentation, such as binary formation.

4.1 SIMULATIONS OF DISC FRAGMENTATION

Simulations of the collapse and fragmentation of rotating isothermal clouds in which fragmentation takes place in flat discs have been carried out by Larson (1978), Wood (1981, 1982) and Miyama *et al.* (1984), all using finite-particle schemes to model the gas dynamics. The predicted length and mass scales for fragmentation depend on the disc surface density, and since later comparisons with observations will be based on average cloud surface densities defined by $M/\pi R^2$ where R is the cloud radius, we use the same definition for the simulations. To minimize the effect of a large change in surface density during the collapse, we restrict attention to calculations made with β_0, the initial ratio of rotational to gravitational energy, equal to 0.3; gravity is then initially nearly balanced by rotation, and the radius of the resulting disc is nearly equal to the initial cloud radius. We can then use the initial radius R to calculate the average surface density of the disc. The sound speed c, which remains constant during the collapse, can be

expressed in terms of the initial ratio $\alpha_0 = 5c^2R/2GM$ of thermal to gravitational energy. The predicted critical mass M_c for the resulting disc can then be calculated from c and the average disc surface density using equation (12). The result, expressed in terms of the number $N = M/M_c$ of critical masses contained in the cloud, is

$$N = 0.43\alpha_0^{-2}. \tag{35}$$

This predicted number should agree, within a factor of order unity, with the number of fragments found in the simulations for different values of α_0. We adopt the number of fragments as the quantity to compare with theory because it can be determined much more unambiguously than the characteristic size or mass of the fragments.

All of the above authors made calculations for $\alpha_0 = 0.4$, 0.3, and 0.2, and the numbers of critical masses predicted by equation (35) for these three cases are 2.7, 4.8, and 10.7. For comparison, in the simulations of both Larson (1978) and Wood (1981, 1982), the numbers of fragments found in the three cases were about 1, 2, and 3–4 respectively. These results scale approximately with the predicted values of N, being about a factor of 2–3 smaller. The simulations of Miyama *et al.* (1984) yielded larger numbers of fragments which are closer to the predicted values of N, i.e. 3, 6, and 8 in the three cases. The closer agreement of these results with the predictions may be partly fortuitous because the discs formed in the simulations of Miyama *et al.* (1984) became more strongly centrally condensed before fragmenting, and most of the fragmentation occurred in the dense central region. In any case, there is at least good qualitative agreement between the theoretical predictions and the numerical simulations, and it appears that equation (35) is able to predict the number of fragments formed within a factor of 2 or 3.

In an early simulation of the fragmentation of an infinitely thin disc, Quirk (1973; unpublished) obtained results qualitatively very similar to the recent 3-dimensional results of Miyama *et al.* (1984), including the formation of dense condensations and numerous spiral filaments. This confirms the expected similarity in the behaviour of infinitely thin and finite-thickness discs, and confirms in particular that the fragmentation of discs is essentially a two-dimensional process.

4.2 FRAGMENTATION OF FILAMENTS AND RINGS

The fragmentation of filaments has been studied numerically by Larson (1972) and Bastien (1983), both of whom found that an isothermal cylinder can fragment into two clumps if the ratio of length to diameter is large enough. For an equilibrium isothermal cylinder, the critical wavelength for fragmentation is 3.94 times the scale radius R defined by equation (20), so one might expect fragmentation to be possible if the length of the cylinder exceeds about four times its radius, or two times its diameter. Bastien (1983) found that fragmentation is marginal when the ratio of length to diameter is two, but very marked when this ratio is five. Again it appears that there is at least rough agreement between theory and simulations, but more comparisons would be desirable.

Many calculations of the collapse of initially axisymmetric clouds have shown the formation of rings, which may subsequently fragment into clumps (Bodenheimer 1981). Although rings probably form only when a high degree of axial symmetry is imposed, they should fragment in much the same way as non-rotating filaments. The fragmentation of one such numerically produced isothermal ring was studied in detail by Norman & Wilson (1978), and from their results it is possible to compare both the separation and the masses of the fragments with theoretical predictions. In the example studied, the circumference of the ring is about three times the predicted wavelength of the fastest growing mode; in good agreement with this prediction, Norman & Wilson found that the highest growth rate occurs for modes containing about 2.5 fragments. Also, the typical fragment masses agree within a factor of 1.5 with the critical mass

calculated from the maximum surface density of the ring using equation (21). For a rather thinner numerically produced ring, Gingold & Monaghan (1983) found breakup into five fragments, again in approximate agreement with theoretical predictions.

5 Critical masses in interstellar clouds

5.1 CLOUD TEMPERATURES

Since the critical mass for a cloud with a given surface density is proportional to c^4 or T^2, an accurate knowledge of cloud temperatures is essential for predicting critical masses. The dependence of temperature on density also plays a crucial role in determining how far fragmentation can continue (see Section 7). To determine the appropriate temperature–density relation, we have collected a number of observational and theoretical results for the temperatures of interstellar clouds as a function of density, and these results are plotted in Fig. 2. The dots with error bars indicate the logarithmic averages and standard deviations of the measured cloud temperatures given in the extensive compilation of data by Myers (1978), binned here into six density ranges. The dashed curve shows the result of a recent theoretical calculation by Boland & de Jong (1984), and the solid curve is based on the semi-empirical temperature–density–opacity relation of Tarafdar *et al.* (1985). The latter curve has been derived from equation (11) of Tarafdar *et al.* by assuming that the visual exitinction A_V is that of a cloud with an equilibrium sheet-like structure. The dot-dash curve shows the result of the simplified theoretical calculation of Larson (1973), included here because it extends to higher densities and includes cooling by dust grains, an effect which dominates the thermal balance at densities above about $10^{-19}\,\mathrm{g\,cm^{-3}}$.

At most densities there is good general agreement among the various theoretical and observational results shown in Fig. 2, and they all exhibit a well-defined trend (with considerable real observational scatter) of decreasing temperature with increasing density up to densities at least as high as $10^{-20}\,\mathrm{g\,cm^{-3}}$. At higher densities the predicted and observed temperatures diverge, the predicted temperature continuing to decrease to a minimum of about 5 K at a density

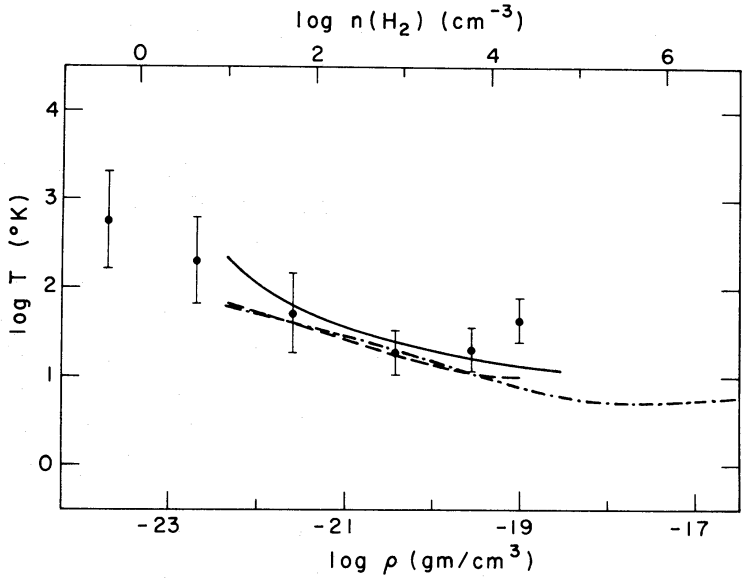

Figure 2. Theoretical and observed temperatures of interstellar clouds as a function of density. Dots with error bars are the logarithmic averages and standard deviations of the measured cloud temperatures compiled by Myers (1978); the solid curve is the semi-empirical temperature–density relation of Tarafdar *et al.* (1985); the dashed curve is the theoretical relation of Boland & de Jong (1984); and the dot-dash curve is the earlier theoretical relation of Larson (1973).

of $2\times10^{-18}\,\mathrm{g\,cm^{-3}}$, while the observed temperatures begin to increase again with increasing density in the densest cloud cores. The reason for this discrepancy is almost certainly that the densest cloud cores are strongly heated by embedded young stellar objects, an effect not included in the theoretical calculations. During the earliest stages of star formation, stellar heating should not yet have become important, so the temperature of a star-forming cloud may continue to decrease to the very low values predicted theoretically. If this is the case, the dependence of temperature on density can be approximated by the power-law relation

$$T\sim17(10^{20}\varrho)^{-0.27} \tag{36}$$

over the entire density range between about 10^{-22} and $10^{-18}\,\mathrm{g\,cm^{-3}}$. This corresponds to a polytropic equation of state with $\gamma=0.73$. We consider in Section 6 cases where stellar heating has become important and this approximation is no longer valid.

5.2 PREDICTED FRAGMENT MASSES

Interpolating in Table 1, we find that for a gas sheet with $\gamma=0.73$, the value of $A(\gamma)$ is 3.6; thus the critical mass from equation (17) is

$$M_c=3.6c(0)^4/G^2\mu. \tag{37}$$

Assuming a mean molecular weight of 2.33 and expressing M_c in solar masses and μ in solar masses per square parsec, this result can be written

$$M_c(M_\odot)=2.4\,T(0)^2/\mu\,(M_\odot\,\mathrm{pc^{-2}}). \tag{38}$$

If we adopt the temperature–density relation (36) and assume that the fragmenting cloud has an equilibrium sheet-like structure with $\varrho(0)=\pi G\mu^2/2c(0)^2$, the critical mass can be expressed as a function only of the surface density μ:

$$M_c(M_\odot)\sim1.6[\mu(M_\odot\,\mathrm{pc^{-2}})/100]^{-2.48}. \tag{39}$$

Since the observed surface densities of interstellar clouds are often expressed in terms of the visual extinction A_V, which in magnitudes is approximately equal to $\mu(M_\odot\,\mathrm{pc^{-2}})/20$, it is also useful to express M_c in terms of A_V:

$$M_c(M_\odot)\sim1.6(A_V/5)^{-2.48}. \tag{40}$$

Equation (40) is valid, if stellar heating is not important, for values of A_V between about 0.3 and 10 mag, corresponding to values of M_c between about 1500 and $0.3\,M_\odot$.

An important result is evident immediately from equation (40): for the values of A_V typically observed in dark clouds, i.e. $A_V\sim5-10$ mag, the predicted critical mass lies in the range ~0.3–$1.6\,M_\odot$. This mass range includes the bulk of the known stars in the solar neighbourhood, and also includes the typical masses of the T Tauri stars observed in dark clouds such as the Taurus clouds. The predicted critical mass is very sensitive to A_V, and almost the entire range of observed stellar masses, $0.3<M_c<85\,M_\odot$, is covered for values of A_V between 1 and 10. This rapid decrease of M_c with increasing A_V is due principally to the decrease of temperature with increasing density implied by equation (36).

The fact that the present results of stability theory lead directly from observed cloud properties to critical masses of stellar order supports the view that stars form by the fragmentation of sheet-like or filamentary structures. Also, it suggests that the fragmentation of molecular clouds is basically a one-stage process, and that extensive hierarchical fragmentation is not important. Herbig (1978) has previously noted that there is, in fact, little evidence from observations that stars form by hierarchical fragmentation.

6 Comparisons with observations

The best comparisons between predicted masses and the observed masses of protostellar clumps and young stars can be made for the nearby Taurus dark clouds, a region of active low-mass star formation where stellar heating apparently plays little role and the measured gas temperature is everywhere close to the 10 K typical of dark clouds. For several of the larger Taurus clouds such as B7, B19, and B22, the average surface densities calculated from the data compiled by Larson (1981) are typically about $160\,M_\odot\,\mathrm{pc}^{-2}$, implying from equation (38) a critical mass of about $1.5\,M_\odot$. For comparison, the dense, apparently protostellar cloud cores studied by Myers & Benson (1983) have masses that are mostly between 0.15 and $4\,M_\odot$, and the median mass of these cores interior to the half-maximum intensity contour is about $0.7\,M_\odot$. (These masses have been corrected downward from those listed by Myers & Benson, which are too large by a factor of 3; I am indebted to P. C. Myers for calling this to my attention.) The median mass of the T Tauri stars in the Taurus clouds is about $0.6\,M_\odot$ (Cohen & Kuhi 1979; Larson 1982), which is very similar to the typical core mass and comparable to, although somewhat smaller than, the predicted critical mass.

The dark clouds and filaments in Taurus have projected separations of the order of 7–14 pc, which may correspond to 3-dimensional separations as large as 28 pc (Kleiner & Dickman 1984); these authors suggest that this dimension may represent a 'fossil Jeans length'. If the Taurus clouds formed by the gravitational fragmentation of an initially sheet-like cloud of atomic hydrogen with the present average surface density of $\sim 30\,M_\odot\,\mathrm{pc}^{-2}$ and a temperature of 80 K, the predicted critical wavelength would be about 10 pc and the most rapidly growing wavelength about 20 pc; these numbers are comparable to the observed separations of the clouds. Also, the predicted critical mass of about $2000\,M_\odot$ is comparable to the masses of the largest dark clouds in the region. Thus the observed sizes and separations of the Taurus clouds are consistent with their having been formed by the fragmentation of a gas sheet. The dense clumps discussed above could then have formed by a later stage of fragmentation made possible by a large drop in temperature (see Section 7).

In most well-studied regions of star formation the observed gas temperature is considerably higher than 10 K, apparently because of heating by embedded or nearby luminous young stars. The effect of a higher temperature is to substantially increase the predicted critical mass; however, typical cloud surface densities are also higher than in Taurus, and this moderates the increase in critical mass. To illustrate these effects, we have used the data on cloud masses and sizes compiled by Larson (1981), together with cloud temperatures from the same original sources, to calculate critical masses for (i) dark clouds, (ii) clouds with reflection nebulae, and (iii) clouds with H II regions. The results for typical dark clouds are essentially the same as for the Taurus clouds. Clouds with reflection nebulae have an average surface density of $230\,M_\odot\,\mathrm{pc}^{-2}$ and an average temperature of 24 K, implying a critical mass of $6\,M_\odot$. Clouds with H II regions have an average surface density of $300\,M_\odot\,\mathrm{pc}^{-2}$ and an average temperature of 38 K, implying a critical mass of $12\,M_\odot$. Although the surface density and temperature both increase systematically along this sequence, the effect of the increase in temperature is much more important, and it causes the predicted critical mass to increase by nearly an order of magnitude from typical dark clouds to typical clouds with H II regions.

The OMC1–OMC2 core region of the Orion molecular cloud is an intensively studied region of formation of massive stars whose properties are relatively extreme compared with those of most clouds with H II regions: the average surface density is about $900\,M_\odot\,\mathrm{pc}^{-2}$, the temperature is about 75 K, and the corresponding critical mass is about $16\,M_\odot$. The temperature quoted here, like those above, is the maximum ^{12}CO brightness temperature, which is an approximate measure of the gas temperature in the 'hot core' region of the cloud. The dense clumps observed by Batrla

et al. (1983) in the OMC1–OMC2 region have masses ranging from 5 to 100 $M_\odot$, and their median mass is $\sim 20\,M_\odot$, again very similar to the predicted critical mass. While the close agreement between the critical mass and the median clump mass is probably fortuitous, it is almost certainly significant that both theory and observation indicate that the typical fragment mass is an order of magnitude larger in the OMC1–OMC2 region than in the Taurus clouds. This difference can be understood as a consequence primarily of the higher temperature in the Orion cloud.

The typical masses of the young stars in the Orion core region also appear to be higher than in Taurus. For example, the median mass of the known T Tauri stars in the Trapezium cluster is $\sim 1.2\,M_\odot$, compared with a median T Tauri mass of $0.6\,M_\odot$ in Taurus (Cohen & Kuhi 1979; Larson 1982). The flare stars in Orion also appear to be systematically more massive than in Taurus, and Orion contains numerous OB stars with masses extending up to a maximum of $42\,M_\odot$, compared with a maximum stellar mass of $8\,M_\odot$ in Taurus (Larson 1982). While these data do not conclusively establish that Orion has a different initial mass function than Taurus, the apparent differences are at least qualitatively in the sense expected from the larger predicted and observed clump masses in Orion.

While the properties of the OMC1–OMC2 region are relatively extreme compared with other nearby regions of star formation, they are by no means extreme on a galactic scale. The well-studied molecular cloud Sgr B2 near the galactic centre has a surface density of about $1800\,M_\odot\,\mathrm{pc}^{-2}$ and a peak temperature of ~ 250 K, and it contains very massive clumps with masses $>500\,M_\odot$ (Wilson *et al.* 1982; Vogel *et al.* 1984). The predicted critical mass is about $85\,M_\odot$, much larger than in any nearby molecular cloud. Again it is clear that the cloud temperature is the dominant factor determining the mass scale for fragmentation. The Sgr B2 cloud is a site of active formation of very massive stars and contains approximately 15 stars of spectral type earlier than O7 (Benson & Johnston 1984), compared with only one such star in Orion.

7 Limits on continuing fragmentation

A question that still needs to be better understood is to what extent a cloud fragment, once formed, can subdivide further into yet smaller objects. The existing numerical simulations of isothermal collapse and fragmentation have so far shown little indication of successive fragmentation, and the fact that the masses of the young stars in Taurus are similar to the masses of the dense cloud cores is consistent with only minimal continuing fragmentation, perhaps involving only the formation of binary and small multiple systems. However, the observed dark clouds and filaments may themselves have been formed by a gravitational fragmentation process, in which case further stages of fragmentation must have occurred to form the protostellar clumps. Continuing fragmentation is likely to be more important during the early stages of cloud condensation, while the temperature is still decreasing with increasing density, than during the later nearly isothermal stages; this is because during early stages the critical mass decreases rapidly with increasing surface density, varying approximately as $\mu^{-2.5}$ according to equation (39), while during isothermal contraction M_c varies only as μ^{-1}. It will be shown below that if rotation is important, continuing fragmentation may even be prevented altogether in the isothermal case, while there is no corresponding limit on continuing fragmentation if the temperature decreases with increasing density.

If a fragment of a uniform, rigidly rotating gas sheet collapses isothermally and axisymmetrically with detailed conservation of angular momentum to form an equilbrium disc, the structure of this disc can be described analytically by the self-similar isothermal disc models of Toomre (1982) and Hayashi *et al.* (1982). The stability parameter Q for such discs has the same value at all radii, and is related to the dimensionless conserved parameter $(G/c)\,dM/dh$, where dM/dh is the mass per unit specific angular momentum (Larson 1984). This quantity in turn is

related to the stability parameter Q_0 of the initial uniformly rotating gas sheet:

$$(G/c)\,dM/dh = 2/Q_0. \tag{41}$$

Using equation (41) and equations (9) and (10) of Larson (1984), the final value of Q can then be calculated given the initial value Q_0. It is found that for all values of Q_0, $Q > 2^{1/2}Q_0$; therefore the final configuration is always significantly more strongly stabilized by rotation than the initial configuration.

If rotation is sufficiently important initially, i.e. if Q_0 is large enough, the final configuration will be completely stable against further fragmentation. If the criterion for stability of an isothermal disc against fragmentation is $Q > 0.75$, as found empirically by Miyama *et al.* (1984), then the final configuration is stable if the initial configuration has $Q_0 > 0.49$. The values of Q and Q_0 required to stabilize the final disc are even smaller if a magnetic field is present; the required value of Q^2 is reduced approximately by an amount p^2, according to equation (33). Further fragmentation becomes more likely for smaller values of Q_0 or β_0 (note that $Q_0 = (32\alpha_0\beta_0/15)^{1/2}$ for a spherical initial configuration), but for very small initial rotation rates fragmentation is suppressed again by the increasing opacity at the centre of the cloud, and in a sufficiently slowly rotating cloud only a single object is formed (Boss 1985).

Qualitatively different results are obtained if the temperature decreases with increasing density, as predicted for example by equation (36). The resulting disc will then still have approximately the same radial distribution of surface density as in the isothermal case, i.e. $\mu \propto r^{-1}$, but it will have a smaller value of Q for a given Q_0; moreover, because the temperature decreases with increasing density and decreasing radius, Q will also decrease inward, varying as $r^{0.37}$ if the temperature follows equation (36). As a result, even if Q is large enough in the outer part of the disc to ensure stability, there will always be an inner region with small Q that is unstable to fragmentation. Hence, in contrast to the isothermal case, continuing fragmentation cannot be prevented as long as the temperature continues to decrease with increasing density.

The detailed thermal behaviour of a fragmenting cloud may therefore play a crucial role in determining the extent to which fragmentation can continue. Fragmentation seems likely to continue as long as the temperature keeps decreasing with increasing density, but further fragmentation becomes less likely and may stop altogether if the temperature becomes constant or begins to rise again, as suggested by Fig. 2. Thus the density at which the temperature reaches its minimum value in a contracting cloud may mark the highest density at which fragmentation is probable, and may determine the minimum likely mass for objects that can form by the direct fragmentation of the cloud. If stellar heating effects are not important, the predicted temperature reaches a minimum value of about 5 K at a density of $\sim 2 \times 10^{-18}$ g cm^{-3}, at which point the critical mass is about $0.3\,M_\odot$. Thus we might expect continuing fragmentation to become progressively less likely for masses below about $0.3\,M_\odot$, producing a peak in the IMF at a mass of this order. If the minimum gas temperature $T_{\min}$ is increased above 5 K by stellar heating or other effects, the predicted minimum fragment mass is also increased, possibly by a large factor; if the temperature at lower densities is still given by equation (36), the predicted minimum mass becomes about $0.3(T_{\min}/5)^{3.35}\,M_\odot$.

We recall that the solar-neighbourhood IMF appears to peak at a mass near $0.3\,M_\odot$ and to fall off rapidly below $0.2\,M_\odot$ (Scalo 1985a, b), in agreement with the above prediction for the case where stellar heating is not important. In some regions of active star formation the IMF appears to peak at a much higher mass (Rieke *et al.* 1980; Jensen, Talbot & Dufour 1981), as would be expected if the minimum gas temperature in these regions has been significantly increased by heating effects associated with the high star formation rate. There is some evidence that the molecular gas in M82, one of the galaxies studied by Rieke *et al.* (1980), has an exceptionally high typical temperature of >40 K (Young & Scoville 1984), implying a critical mass $>10\,M_\odot$ and hence a large typical stellar mass, according to the above arguments.

8 Conclusions

Theoretical arguments and numerical simulations both suggest that fragmentation is not likely to be significant during the free collapse of an initially nearly uniform cloud. Instead, either rotation, a magnetic field, or initial anisotropy will in general cause the cloud to collapse toward a flattened or filamentary configuration which appoaches hydrostatic equilibrium in at least one dimension. Once overall collapse has been halted and approximate equilibrium has been established, at least locally, gravitational instability can cause the resulting sheet or filament to break into fragments of a characteristic size determined by its scale height.

The characteristic mass of the fragments depends on the temperature and surface density of the cloud, and is approximately the same for both sheets and filaments; thus the mass scale for fragmentation is not sensitive to the detailed 3-dimensional structure of the cloud. The fragment mass is also not significantly altered by the presence of rotation or a magnetic field, although either rotation or a magnetic field could, if important enough, prevent fragmention altogether. The results presented in Section 2 for the stability of equilibrium sheets and filaments should therefore apply fairly generally to the fragmentation of interstellar clouds. A number of numerical simulations of the fragmentation of discs, filaments, and rings have yielded results compatible with these theoretical predictions.

In two well-studied regions of star formation, the Taurus dark clouds and the OMC1–OMC2 region in Orion, the predicted critical masses agree well with the typical observed masses of the densest molecular clumps. The median mass of the T Tauri stars in the Taurus dark clouds is also very similar to the typical clump mass, and comparable to the predicted critical mass. In the OMC1–OMC2 region, the critical mass and the typical clump mass are both about an order of magnitude larger than in the Taurus clouds. An important conclusion is that the differences in the fragment masses in different regions of star formation can be understood as due primarily to differences in the gas temperature; differences in surface density are of secondary importance. Thus the temperature appears to be the dominant factor controlling the mass scale for fragmentation. If heating by luminous young stars is not important and the temperature becomes as low as expected theoretically, critical masses as small as $\sim 0.3\,M_\odot$ are predicted; however, if stellar heating is important, as in the vicinity of H II regions, the critical mass rises substantially to values exceeding $10\,M_\odot$.

If rotation is important, it exerts an inhibiting effect on continuing fragmentation, and in the isothermal case it may completely prevent a cloud fragment from breaking up further into smaller objects. However, continuing fragmentation cannot be prevented as long as the temperature decreases with increasing density, as is expected to occur during the early low-density stages of evolution of star-forming clouds. Thus the detailed dependence of temperature on density may be crucial in determining the extent to which fragmentation can continue, and hence the form of the stellar initial mass function. In the absence of stellar heating effects, the predicted gas temperature keeps decreasing until the critical mass is about $0.3\,M_\odot$, so fragmentation may stop at a mass of this order. The IMF of solar-neighbourhood stars does, in fact, appear to peak at a mass of about $0.3\,M_\odot$. If the minimum gas temperature is increased by stellar heating or other effects, the mass at which the IMF peaks could be much larger.

These arguments suggest that the stellar IMF need not be a universal function, and may in fact vary strongly, depending on the temperature of the star-forming cloud. It is possible, for example, that the IMF depends on the local rate of star formation, the typical stellar mass being higher in regions with high star formation rates because of the heating effects of the young stars. This effect could cause the IMF to vary with both space and time in galaxies, the typical stellar mass being larger at earlier times and in denser regions, reflecting the expected variations in the star formation rate. Some of the possible implications of such non-standard initial mass functions will be explored in a subsequent paper.

References

Bardeen, J. M., 1971. *Astrophys. J.*, **167,** 425.
Bastien, P., 1983. *Astr. Astrophys.*, **119,** 109.
Batrla, W., Wilson, T. L., Bastien, P. & Ruf, K., 1983. *Astr. Astrophys.*, **128,** 279.
Benson, J. M. & Johnston, K. J., 1984. *Astrophys. J.*, **277,** 181.
Bodenheimer, P., 1981. *Fundamental Problems in the Theory of Stellar Evolution, IAU Symp. No. 93*, p. 5, eds Sugimoto, D., Lamb, D. Q. & Schramm, D. N., Reidel, Dordrecht, Holland.
Boland, W. & de Jong, T., 1984. *Astr. Astrophys.*, **134,** 87.
Boss, A. P., 1985. *Icarus,* **61,** 3.
Chandrasekhar, S. & Fermi, E., 1953. *Astrophys. J.*, **118,** 116.
Cohen, M. & Kuhi, L. V., 1979. *Astrophys. J. Suppl.*, **41,** 743.
Elmegreen, B. G. & Elmegreen, D. M., 1978. *Astrophys. J.*, **220,** 1051.
Gingold, R. A. & Monaghan, J. J., 1983. *Mon. Not. R. astr. Soc.*, **204,** 715.
Goldreich, P. & Lynden-Bell, D., 1965a. *Mon. Not. R. astr. Soc.*, **130,** 97.
Goldreich, P. & Lynden-Bell, D., 1965b. *Mon. Not. R. astr. Soc.*, **130,** 125.
Harrison, E. R. & Lake, R. G., 1972. *Astrophys. J.*, **171,** 323.
Hayashi, C., Narita, S. & Miyama, S. M., 1982. *Prog. Theor. Phys.*, **68,** 1949.
Herbig, G. H., 1978. *The Origin of the Solar System*, p. 219, ed. Dermott, S. F., Wiley, New York.
Hoyle, F., 1953. *Astrophys. J.*, **118,** 513.
Hunter, C., 1964. *Astrophys. J.*, **139,** 570.
Hunter, C., 1972. *Ann. Rev. Fluid Mech.*, **4,** 219.
Jeans, J. H., 1929. *Astronomy and Cosmogony*, Cambridge University Press (reprinted by Dover, New York, 1961).
Jensen, E. B., Talbot, R. J. & Dufour, R. J., 1981. *Astrophys. J.*, **243,** 716.
Kleiner, S. C. & Dickman, R. L., 1984. *Astrophys. J.*, **286,** 255.
Larson, R. B., 1972. *Mon. Not. R. astr. Soc.*, **156,** 437.
Larson, R. B., 1973. *Fundam. Cosmic Phys.*, **1,** 1.
Larson, R. B., 1978. *Mon. Not. R. astr. Soc.*, **184,** 69.
Larson, R. B., 1981. *Mon. Not. R. astr. Soc.*, **194,** 809.
Larson, R. B., 1982. *Mon. Not. R. astr. Soc.*, **200,** 159.
Larson, R. B., 1984. *Mon. Not. R. astr. Soc.*, **206,** 197.
Layzer, D., 1963. *Astrophys. J.*, **137,** 351.
Ledoux, P., 1951. *Ann. d'Astrophys.*, **14,** 438.
Mestel, L., 1965. *Q. Jl. R. astr. Soc.*, **6,** 161 and 265.
Miyama, S. M., Hayashi, C. & Narita, S., 1984. *Astrophys. J.*, **279,** 621.
Myers, P. C., 1978. *Astrophys. J.*, **225,** 380.
Myers, P. C. & Benson, P. J., 1983. *Astrophys. J.*, **266,** 309.
Nakano, T., 1984. *Fundam. Cosmic Phys.*, **9,** 139.
Nakano, T. & Nakamura, T., 1978. *Publs astr. Soc. Japan,* **30,** 671.
Nakamura, T., 1983. *Prog. Theor. Phys.*, **70,** 747.
Nakamura, T., 1984. *Prog. Theor. Phys.*, **71,** 212.
Norman, M. L. & Wilson, J. R., 1978. *Astrophys. J.*, **224,** 497.
Ostriker, J., 1964. *Astrophys. J.*, **140,** 1056.
Ostriker, J., 1965. *Astrophys. J. Suppl.*, **11,** 167.
Pacholczyk, A. G., 1963. *Acta Astronomica,* **13,** 1.
Quirk, W. J., 1973. *Bull. Am. astr. Soc.*, **5,** 9.
Rieke, G. H., Lebofsky, M. J., Thompson, R. I., Low, F. J. & Tokunaga, A. T., 1980. *Astrophys. J.*, **238,** 24.
Rozyczka, M., 1983. *Astr. Astrophys.*, **125,** 45.
Scalo, J. M., 1985a. *Astr. J.*, **90,** in press.
Scalo, J. M., 1985b. *Fundam. Cosmic Phys.*, in press.
Schneider, S. & Elmegreen, B. G., 1979. *Astrophys. J. Suppl.*, **41,** 87.
Simon, R., 1965. *Ann. d'Astrophys.*, **28,** 40.
Smith, J. A., 1980. *Astrophys. J.*, **238,** 842.
Spitzer, L., 1942. *Astrophys. J.*, **95,** 329.
Spitzer, L., 1978. *Physical Processes in the Interstellar Medium*, Wiley, New York.
Stodolkiewicz, J. S., 1963. *Acta Astronomica,* **13,** 30.
Tarafdar, S. P., Prasad, S. S., Huntress, W. T., Villere, K. R. & Black, D. C., 1985. *Astrophys. J.*, **289,** 220.
Tohline, J. E., 1980a. *Astrophys. J.*, **235,** 866.
Tohline, J. E., 1980b. *Astrophys. J.*, **239,** 417.

Toomre, A., 1964. *Astrophys. J.,* **139,** 1217.
Toomre, A., 1981. *The Structure and Evolution of Normal Galaxies*, p. 111, eds Fall, S. M. & Lynden-Bell, D., Cambridge University Press.
Toomre, A., 1982. *Astrophys. J.,* **259,** 535.
Vogel, S. N., Genzel, R., Ho, P. T. P. & Palmer, P., 1984. *Bull. Am. astr. Soc.,* **16,** 462.
Wilson, T. L., Ruf, K., Walmsley, C. M., Martin, R. N., Pauls, T. A. & Batrla, W., 1982. *Astr. Astrophys.,* **115,** 185.
Wood, D., 1981. *Mon. Not. R. astr. Soc.,* **194,** 201.
Wood, D., 1982. *Mon. Not. R. astr. Soc.,* **199,** 331.
Young, J. S. & Scoville, N. Z., 1984. *Astrophys. J.,* **287,** 153.